Enhanced Ferroelectric Polarization by Induced Dy Spin Order in Multiferroic $DyMnO_3$

O. Prokhnenko,[1] R. Feyerherm,[2] E. Dudzik,[2] S. Landsgesell,[1] N. Aliouane,[1] L. C. Chapon,[3] and D. N. Argyriou[1]

[1]*Hahn-Meitner-Institut, Glienicker Strasse 100, D-14109 Berlin, Germany*

[2]*Hahn-Meitner-Institut, c/o BESSY, D-12489 Berlin, Germany*

[3]*ISIS, Rutherford Appleton Laboratory, Chilton, Didcot, OX11, 0QX United Kingdom*

(Received 3 September 2006; published 1 February 2007)

Neutron powder diffraction and single crystal x-ray resonant magnetic scattering measurements suggest that Dy plays an active role in enhancing the ferroelectric polarization in multiferroic $DyMnO_3$ above $T_N^{Dy} = 6.5$ K. We observe the evolution of an incommensurate ordering of Dy moments with the same periodicity as the Mn spiral ordering. It closely tracks the evolution of the ferroelectric polarization. Below T_N^{Dy}, where Dy spins order commensurately, the polarization decreases to values similar for those of $TbMnO_3$. The higher P_s found just above T_N^{Dy} arises from the contribution of Dy spins so as to effectively increase the amplitude of the Mn spin spiral.

DOI: 10.1103/PhysRevLett.98.057206 PACS numbers: 75.30.Kz, 61.10.−i, 61.12.Ld, 77.80.Fm

The strong coupling between ferroelectricity and magnetism in modern multiferroics has offered a new paradigm of magneto-electric materials. It has stimulated a search for new multiferroics and highlighted the need for a deeper understanding of the physics behind these exciting materials. Although the requirements of magnetism and ferroelectricity are chemically incompatible [1], in these new multiferroics spin frustration [2] leads to complex magnetic arrangements that can break inversion symmetry [3,4]. The strong coupling provided by frustration in the perovskite manganites $RMnO_3$ leads to a number of magneto-electric phenomena. For example, compounds with $R =$ Tb and Dy exhibit flops of the direction of the spontaneous polarization ($\mathbf{P}_s$) with applied field ($\mathbf{H}$) while ferroelectricity is observed only under a magnetic field in $R =$ Gd [3,5–7]. Of these, $R =$ Dy exhibits the largest value of $P_s \sim 0.2\ \mu C/cm^2$ (more than 3 times larger than that for $R =$ Tb) and a giant magnetocapacitance effect [6].

In these materials, a phenomenological treatment of the coupling of a uniform electric polarization $\mathbf{P}$ to an inhomogeneous magnetization $\mathbf{M}$ leads to a term linear in the gradient $\nabla\mathbf{M}$, the so-called Lifshitz invariant, that is allowed in states with broken inversion symmetry [8]. This model is consistent with neutron diffraction experiments on $TbMnO_3$ that showed that a spiral arrangement of Mn spins within the bc plane develops at $T_l = 28$ K, coinciding with the onset of $\mathbf{P}_s$ [9]. Although in this picture the contribution to $\mathbf{P}_s$ from the magnetic ordering of R ions is ignored, their role is underscored as a source of magnetic anisotropy that is required to predict the correct direction of $\mathbf{P}_s$ under an applied magnetic field [8].

In this Letter we present measurements on $DyMnO_3$ demonstrating that Dy spin ordering significantly contributes to P_s above $T_N^{Dy} = 6.5$ K. We have combined neutron powder diffraction and single crystal x-ray resonant magnetic scattering to investigate the evolution of magnetism with temperature. We find that the Dy spins order along the b axis in a sinusoidal incommensurate (ICM) structure with the same periodicity as Mn spins below $T_l^{Dy} = 15$ K. On further cooling P_s rises to values approximately twice those found for the maximum P_s in $TbMnO_3$. The commensurate (CM) Dy ordering below T_N^{Dy} results in an abrupt decrease in P_s, while the CM-ICM transition shows a large hysteresis in which P_s and the intensity of ICM Dy magnetic scattering exhibit a similar behavior. Extending the phenomenology for multiferroics [8] we can account quantitatively for the enhancement of P_s just above T_N^{Dy} based on our determination of the Dy spin ordering, thus demonstrating for the first time how R spins can enhance significantly the polarization of these novel multiferroic perovskites.

For $R =$ Dy below $T_N \sim 39$ K, Mn spins are expected to order first along the b axis in an ICM sinusoidal arrangement with propagation vector $\boldsymbol{\tau}^{Mn} = (0\ 0.36 \ldots 0.385\ 0)$ obtained on the basis of lattice reflections with $q = 2\tau$ [2,7,10] that arise from a coupling of the ICM magnetic ordering to the lattice via a quadratic magneto-elastic coupling [11]. Below $T_l = 28$ K for $R =$ Tb, an additional component of the Mn magnetic moment along the c axis, in phase quadrature with the component along b, gives rise to a spiral magnetic ordering and breaks inversion symmetry, leading to the observation of $\mathbf{P}_s$ along the c axis. A similar transition occurs for $R =$ Dy at $T_l = 18$ K [6] as illustrated in Fig. 1(a). Below T_N^{Dy} Dy magnetic moments order separately with propagation vectors $\tau^{Dy} = (0\ \frac{1}{2}\ 0)$ [10].

To investigate the evolution of the magnetic ordering of $DyMnO_3$ with neutron powder diffraction (NPD) we used a 0.65 g polycrystalline $^{162}DyMnO_3$ sample prepared from a mixture of isotope enriched $^{162}Dy_2O_3$ oxide (94.4% enrichment) and Mn_2O_3, using standard solid state synthesis methods. Isotopic ^{162}Dy was chosen for its smaller neutron absorption cross section (σ_a) compared to that of natural Dy [12]. NPD data were measured from this sample between 2–300 K on the GEM diffractometer at the ISIS facility, Rutherford-Appleton Laboratory. The data were analyzed with the FullProf refinement package [13].

 © 2007 The American Physical Society

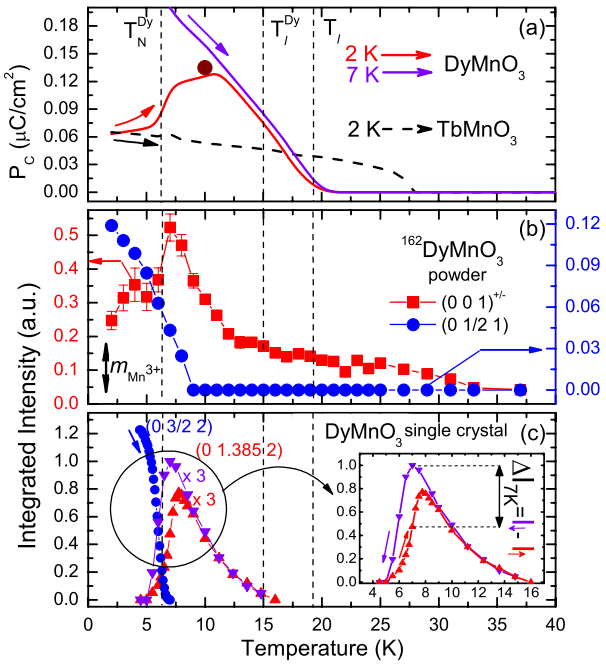

FIG. 1 (color online). Temperature dependences of (a) electric polarization along the c axis for $DyMnO_3$ and $TbMnO_3$ (from Goto *et al.* [6]), (b) integrated (neutron) intensities of magnetic A-type and $(0\ \frac{1}{2}\ 1)$ reflections measured on heating ($\updownarrow m_{Mn^{3+}}$ shows the intensity corresponding to a $4\mu_B Mn^{3+}$ magnetic moment for this reflection), (c) temperature dependent integrated (synchrotron) intensities of selected Dy commensurate (heating) and incommensurate (heating and cooling) superlattice reflections. The region around T_N^{Dy} is shown in the inset. Here, ΔI highlights the difference between intensities on cooling and heating at 7 K. The symbol ● in panel (a) represents the prediction of P at 10 K for R = Dy on the basis of the ordering of both Mn and Dy spins determined by neutron diffraction (see text).

Synchrotron x-ray diffraction measurements on a $DyMnO_3$ single crystal were conducted at the 7 T multipole wiggler beam line MAGS, operated by the Hahn-Meitner-Institut at the synchrotron source BESSY in Berlin. Details on the crystal growth, beam line, and experimental procedure have been reported previously [10,14]. Low field (500 Oe) magnetization of the polycrystalline and single crystal samples was measured in a SQUID magnetometer between 4—100 K. The data showed $T_N^{Dy} = 9$ and 6 K for the polycrystalline and single crystal sample, respectively. The value of T_N^{Dy} of our single crystal is in good agreement with published data [2] and may suggest that the higher value obtained for the powder sample may arise from a small nonstoichiometry, as suggested by a difference in the lattice constants between these two samples at 300 K [10].

Turning first to the NPD measurements we found that $^{162}DyMnO_3$ crystallized with the orthorhombically distorted perovskite structure (space group $Pbnm$). Cooling the sample below $T_N \sim 40$ K we find a series of magnetic satellites arising from Mn spin ordering [see Fig. 2(a)] similar to the observations of Quezel *et al.* [15] on $TbMnO_3$. Using their notation, these $(hkl) \pm \tau$ reflections are characterized as A type where $h + k$ = even and l = odd and $\tau = (0\ \tau_y^{Mn}\ 0)$ is an incommensurate propagation vector along the b^* axis. An increase of satellite intensities (and τ_y^{Mn}) with decreasing temperature is accompanied by the appearance of G-type satellites ($h + k$ = odd and l = odd) below ~15 K, where a nonzero value of P_s is observed as shown in Fig. 1(a) [6,7]. Below T_N^{Dy} the NPD data show an intensity reduction of the A-type satellites, which coincides with the appearance of a CM Dy magnetic order with propagation vector $\tau^{Dy} = (0\ \frac{1}{2}\ 0)$ [see Figs. 1(b) and 2(a)] [10]. This transition coincides with a sharp decrease of P_s. The G-type reflections are too weak for a quantitative comparison. Rietveld analysis of the NPD data between $T_N^{Dy} < T < 13$ K on the assumption of pure Mn spin ordering (see below) leads to unphysically large moments for Mn^{3+} ($>4\mu_B$/Mn) [Fig. 1(b)]. The rapid increase of the magnetic intensity below 13 K [shaded area in Fig. 1(b)] and its decrease below T_N^{Dy} suggests an additional magnetic contribution to the intensity of these reflections from Dy. As can be seen in Fig. 2(a), the magnetic reflections are relatively broad and below (Fig. 3, caption) we shall argue that this probably arises from a distribution of the propagation vectors.

In order to probe directly the magnetic contribution of Dy to the intensities of these ICM magnetic reflections, we

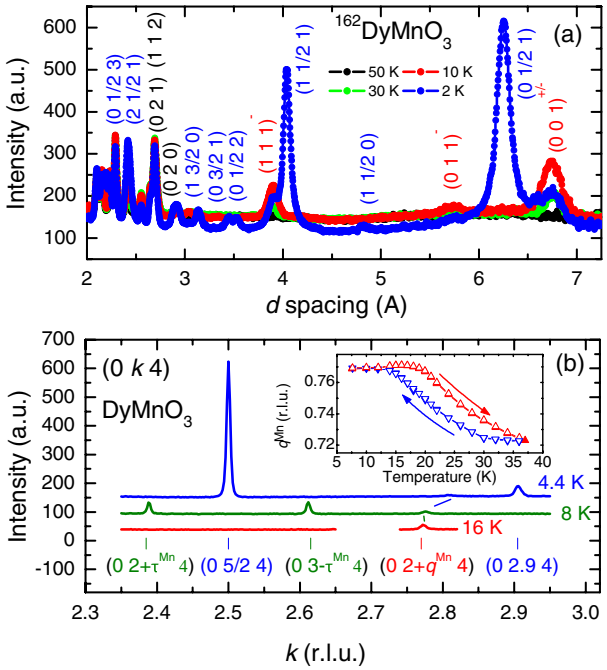

FIG. 2 (color online). (a) Neutron diffraction patterns obtained from the 24°–45° bank of the GEM diffractometer at 2, 10, 30, and 50 K. (b) k scans along $(0\ k\ 4)$ at various temperatures measured with a synchrotron x-ray energy close to the Dy-L_3 absorption edge. No polarization analysis was employed here in order to allow for simultaneous observation of structural and magnetic superstructure reflections. Inset: temperature dependence of the lattice modulation wave vector obtained from a superstructure reflection of type $(0\ k\ 3)$.

have used single crystal resonant x-ray scattering at an x-ray energy of 7.794 keV, slightly above the Dy-L_3 absorption edge. With this resonant condition, a survey of reciprocal space was carried out at different temperatures. Figure 2(b) shows scans along the (0 k 0) direction as examples. At 16 K only the Mn induced structural modulation q^{Mn} is observed, producing the (0 2.77 4) Bragg reflection. At 8 K a pair of relatively strong additional (0 2.385 4) and (0 2.615 4) reflections appears, consistent with the magneto-elastic coupling $q^{\mathrm{Mn}} = 2\tau^{\mathrm{Mn}}$. At 4.4 K the latter reflections have disappeared, in contrast to the associated peak from the Mn induced structural modulation that decreases in intensity and is shifted towards a q_y^{Mn} value of 0.81. The extinct reflections are replaced by significantly stronger Bragg reflections at (0 2.5 4) and (0 2.905 4) which correspond to the CM magnetic ordering of the Dy moments and the associated incommensurate lattice modulation $q_y^{\mathrm{Dy}} = 0.905 \neq 2\tau_y^{\mathrm{Dy}}$, respectively. This transition has been discussed recently elsewhere [10].

In order to identify the nature of the Bragg reflections associated with τ^{Mn} above T_N^{Dy} we employed linear polarization analysis [10]. Figure 3 shows the dependence of the intensities of both the (0 2.385 4) and the related (0 2.77 4) reflections on the polarization analyzer configuration ($\sigma \rightarrow \sigma'$ versus $\sigma \rightarrow \pi'$) at 8.5 K. The characteristic behavior shows that the former is of magnetic and the latter of structural origin. Tuning the x-ray energy to a value 20 eV below the Dy-L_3 absorption edge leads to a reduction of the intensity of the magnetic (0 2.385 4) reflection measured in $\sigma \rightarrow \pi'$ configuration by a factor of 40. This resonance enhancement shows that the (0 2.385 4) reflection is due to ordered Dy magnetic moments and that any contribution of the ordered Mn moments to this reflection is negligible.

Figure 1(c) shows the temperature dependence of the integrated intensities of two particularly strong Bragg reflections, (0 1.385 2) and (0 1.5 2), related to τ^{Mn} and τ^{Dy}, respectively. The half-integer reflection, associated with the CM magnetic ordering of the Dy moments, vanishes above $T_N^{\mathrm{Dy}} = 6.5$ K. Simultaneously, the intensity of the ICM reflection increases steeply on heating. At the same temperature $\mathbf{P}_s \parallel c$ increases to approximately twice its value compared to that at temperatures just below T_N^{Dy} [Fig. 1(a)]. On further heating, the (0 1.385 2) Bragg intensity passes a maximum around 8 K, decreases monotonically with a concave curvature—typical for an induced magnetic moment, and finally vanishes above $T_l^{\mathrm{Dy}} = 15$ K. In addition, it exhibits a significant hysteresis [see inset in Fig. 1(c)]. On cooling from 16 K, the (0 1.385 2) Bragg intensity measured at 7 K is about twice as large as the intensity obtained on heating from 4.5 to 7 K. Monitoring the count rate at fixed $k = 1.385$ while sweeping the temperature at various rates (0.05 . . . 1 K/ min) we verified that whenever one does not cross T_N^{Dy}, the cooling and heating curves above T_N^{Dy} are reversible and the hysteresis is independent of the heating or cooling rate. This behavior

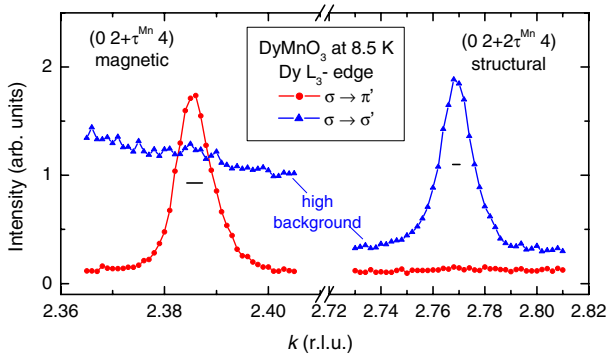

FIG. 3 (color online). Linear polarization analysis of (left) the (0 2.385 4) and (right) the (0 2.77 4) superstructure reflections at 8.5 K. The intensity variation as a function of the polarization analyzer configuration shows that (0 2.385 4) is of magnetic and (0 2.77 4) of structural origin. The linewidths of both reflections are significantly enhanced with respect to the instrumental resolution that is marked by horizontal bars. Since the linewidth of the second order reflection (0 2.77 4) is roughly twice as large as that of the first order (0 2.385 4), the broadening is more likely due to an inhomogeneous distribution of τ values in the sample rather than to reduced coherence lengths.

of Dy induced ordering strongly resembles the hysteresis of the electric polarization shown in Fig. 1(a), where a factor of 2 difference is shown in the cooling and heating curves at 7 K, the same difference that we find in the hysteresis of the intensity of the (0 1.385 2) reflection. Finally, the inset in Fig. 2(b) shows the temperature dependence of q^{Mn} measured in two successive heating and cooling cycles between 7.5 and 40 K. Clearly, a significant hysteresis of about 5 K in width is observed in the temperature dependence. Neither on cooling nor on heating any sharp lock-in transition is observed. The edge of the heating curve, however, is consistent with the reported value for $T_l = 18$ K.

Having directly established the behavior of Dy spins above and below T_N^{Dy} we turn our attention to models of magnetic ordering for Dy that can be obtained from the analysis of the NPD data. In the CM regime below T_N^{Dy} the diffraction data indicate a cell doubling along b arising from antiferromagnetic Dy spin ordering. Rietveld analysis shows that the Dy moments with absolute value $m^{\mathrm{Dy}} = 6.2(6)\mu_B/\mathrm{Dy}$ lie in the ab plane, being canted $30(\pm 10)°$ from the b axis, and are stacked antiferromagnetically along the c axis.

In the analysis of the induced magnetic ordering of Dy spins at 10 K, above T_N^{Dy}, we have taken solutions of the magnetic structure that are allowed by the $\Gamma_2 \otimes \Gamma_3$ representation of the $Pbnm$ space group indicated by the spiral arrangements of Mn spins in $TbMnO_3$ [$\mathbf{m}^{\mathrm{Mn}} = (0, 3.9, 2.8)$] [9,16]. In the case where two irreproducible representations are coupled [9], the R moments are allowed to have components along the three principal crystallographic directions denoted as $\mathbf{m}^{\mathrm{Dy}} = (a_x, f_y, f_z)$ [16]. Our Rietveld analysis shows that the magnetic moment is

$\mathbf{m}^{\mathrm{Dy}} = (0.4(6), 2.5(2), 0.0(3))\mu_B/\mathrm{Dy}$. The maximum value of the moment here is approximately twice as much as that found for the induced moment of Tb in $TbMnO_3$ [$\mathbf{m}^{\mathrm{Tb}} = (1.2, 0, 0)\mu_B/\mathrm{Tb}$ [9]].

The CM structure of Dy spins below T_N^{Dy} preserves the mirror plane perpendicular to the c axis and thus obviously does not allow for a contribution to $\mathbf{P}_s$ along the c axis. Polarization measurements show that this spin ordering also does not contribute to $\mathbf{P}_s$ along the other principal crystallographic directions ($\mathbf{P} \parallel a \sim \mathbf{P} \parallel b \sim 0$) [7]. For the region just above T_N^{Dy} our data are consistent with a sinusoidal modulation of the Dy spins along the b axis. The absence of a c-axis component would exclude the presence of a Dy bc spiral as found for the case of Mn spin ordering in $TbMnO_3$. Thus, on the basis of symmetry the induced Dy spin order *alone* is unlikely to result in a ferroelectric polarization along the c axis above T_N^{Dy}.

In the region just above T_N^{Dy}, P_s is 3 times larger for $R =$ Dy compared to $R =$ Tb or (Eu,Y) compounds and shows a large hysteresis. Indeed, Goto *et al.* [6] find almost a 50% difference in P_s at 7 K obtained after cooling to 2 and 7 K, a behavior that is similar to the hysteresis of the magnetic intensity from the induced Dy spin order [Fig. 1(c)]. Recent phenomenological models [8,9] which describe P_s in terms of the Mn spiral ordering alone do not account for the enhancement of P_s in $DyMnO_3$ just above T_N^{Dy}. Extending the phenomenology of Ref. [8] to include the contribution of a sinusoidal ordering of Dy spins that order with the same wave vector as Mn moment, can quantitatively account for the enhancement of P_s in this region. Here the contribution of Dy spins is included to Eq. (3) of Ref. [8] so that $\mathbf{M} = (m_y^{\mathrm{Mn}} + \epsilon m_y^{\mathrm{Dy}})\mathbf{y}\cos(\boldsymbol{\tau}\cdot\mathbf{y}) + m_z^{\mathrm{Mn}}\mathbf{z}\sin(\boldsymbol{\tau}\cdot\mathbf{y}) + m_x^{\mathrm{Mn}}\mathbf{x}$, where $\mathbf{x}, \mathbf{y}, \mathbf{z}$ are unit vectors along the three principal crystallographic directions a, b, c, respectively, and ϵ is a constant close to 1. Inserting $\mathbf{M}$ in Eqs. (2) and (4) of the same reference gives $\mathbf{P} = \gamma\chi(m_y^{\mathrm{Mn}} + \epsilon m_y^{\mathrm{Dy}})m_z^{\mathrm{Mn}}(\mathbf{y} \times \boldsymbol{\tau})$, where γ and χ are a coupling constant and the susceptibility, respectively. We use this expression with the magnetic structure derived from neutron diffraction for both Mn and R orderings to compare the polarization of $R =$ Tb and Dy in the region of 10–15 K. Taking the values of the magnetic moments for $R =$ Tb from Ref. [9] and for $R =$ Dy from this work we have a value of $P^{\mathrm{Tb}} = 3.1\gamma\chi$ and $P^{\mathrm{Dy}} = 7.9\gamma\chi$. Scaling these values to $P^{\mathrm{Tb}}(10\ \mathrm{K}) \sim 0.055\ \mu\mathrm{C/cm^2}$, we can compute $P^{\mathrm{Dy}}(10\ \mathrm{K}) = 0.135\mu C/\mathrm{cm}^2$, in excellent agreement with the experimental measurements shown in Fig. 1(a), assuming the constants are essentially equal in both compounds. Our work shows that the enhancement in P_s for $R =$ Dy compared to that of $R =$ Tb is associated with the induced ordering of Dy spins along one of the components of the Mn spiral with the same τ. The increase in P_s is achieved by effectively enhancing one of the components of the Mn spiral. The decrease in P_s below T_N^{Dy} we ascribe to the change in the wave vector for the Dy ordering ($\tau^{\mathrm{Dy}} \neq \tau^{\mathrm{Mn}}$) as illustrated in Fig. 1(a). The quantitative agreement we obtain for P_s on the basis of the magnetic structure of the two manganites and the phenomenology attest to the validity of our model and provides for ways to explore increases in the polarization of multiferroic manganites.

In summary, we demonstrate that the induced magnetic ordering of Dy coincides with a region of enhanced polarization compared to other $RMnO_3$ manganites, while below T_N^{Dy} when Dy spins order commensurately P_s is sharply reduced. The higher P_s found just above T_N^{Dy} arises from the contribution of Dy spins so as to effectively increase the amplitude of the Mn spin spiral.

The authors have benefited from discussions with M. Mostovoy and T. Kimura. We also thank an anonymous referee for helpful comments. Construction of the beam line MAGS has been founded by the BMBF via the HGF-Vernetzungsfonds under Contracts No. 01SF0005 and No. 01SF0006. S. L. thanks the DFG for financial support via Contract No. AR 613/1-1.

[1] N. A. Hill, J. Phys. Chem. B **104**, 6694 (2000).
[2] T. Kimura, S. Ishihara, H. Shintani, T. Arima, K. T. Takahashi, K. Ishizaka, and Y. Tokura, Phys. Rev. B **68**, 060403(R) (2003).
[3] T. Kimura, T. Goto, H. Shintani, K. Ishizaka, T. Arima, and Y. Tokura, Nature (London) **426**, 55 (2003).
[4] Th. Lottermoser, T. Lonkai, U. Amann, D. Hohlwein, J. Ihringer, and M. Fiebig, Nature (London) **430**, 541 (2004).
[5] M. Fiebig, J. Phys. D **38**, R123 (2005).
[6] T. Goto, T. Kimura, G. Lawes, A. P. Ramirez, and Y. Tokura, Phys. Rev. Lett. **92**, 257201 (2004).
[7] T. Kimura, G. Lawes, T. Goto, Y. Tokura, and A. P. Ramirez, Phys. Rev. B **71**, 224425 (2005).
[8] M. Mostovoy, Phys. Rev. Lett. **96**, 067601 (2006).
[9] M. Kenzelmann, A. B. Harris, S. Jonas, C. Broholm, J. Schefer, S. B. Kim, C. L. Zhang, S.-W. Cheong, O. P. Vajk, and J. W. Lynn, Phys. Rev. Lett. **95**, 087206 (2005).
[10] R. Feyerherm, E. Dudzik, N. Aliouane, and D. N. Argyriou, Phys. Rev. B **73**, 180401(R) (2006).
[11] M. B. Walker, Phys. Rev. B **22**, 1338 (1980).
[12] For ^{162}Dy, $\sigma_a = 194$ barn while for natural Dy $\sigma_a = 994$ barn, V. F. Sears, Neutron News **3**, 26 (1992).
[13] J. Rodriguez-Carvajal, Physica (Amsterdam) **B192**, 55 (1993).
[14] E. Dudzik, R. Feyerherm, W. Diete, R. Signorato, and C. Zilkens, J. Synchrotron Radiat. **13**, 421 (2006).
[15] S. Quezel, F. Tcheou, J. Rossat-Mignod, G. Quezel, and E. Roudaut, Physica B+C (Amsterdam) **86–88**, 916 (1977).
[16] H. W. Brinks, J. Rodriguez-Carvajal, H. Fjellvag, A. Kjekshus, B. C. Hauback, and E. Dagatto, Phys. Rev. B **63**, 094411 (2001).